

On Thixotropic Effect of Borehole Flow under Steady Flow Rate

Alexander Starostin

Baker Hughes, Baker-Hughes-Straße 1, 29221 Celle, Germany
Alexander.Starostin@bakerhughes.com

Abstract - This paper considers the thixotropic non-Newtonian fluid flow in the duct under steady rate. Such flow occurs after pump start-up while drilling and other industrial processes. We propose a model to describe the influence of gel breaking phenomena on the flow. The fluid structural parameter defines fluid yield point and is a subject of gel build up and strain-dependent gel breaking. A control volume approach with the additional assumption on velocity profile enables the analytical solution. This solution evaluates the evolution of flow structure, as the plug reduces and accelerates and the yielding zone grows from the wall. The offered solution can be used for planning and automation of industrial processes sensitive to gel presence.

Keywords: duct flow, thixotropy, gel breaking

1. Introduction

During borehole drilling the pumps at the surface circulate the drilling mud downwards in the tubing and upwards through the annulus. The flow stops regularly for surface operations. Many types of drilling mud exhibit time-dependent stresses. They build a high viscous gel as the flow stops and turn gradually to less viscous fluid as the flow resumes. A common practice in drilling operations is to ramp up the pumps to a moderate flow rate and keep it constant until gel degrades. After a flow initiation the gel breaking starts in the shear flow region. Pressure dynamics is affected by gel presence (see Figure 1). The gel degradation stage lasts 10-100 seconds, meanwhile pressure gradient falls. The degradation might not completely remove gels in the borehole, but it mitigates high pressure values for high flow rates. Afterwards pumps ramp up to a higher operational flow rate. The principal question for drilling operation is when to finish gel breaking and switch to operational rate. This has motivated us for this study on transient effect in drilling mud flow under steady flow.

The dependence of stress on time is known as thixotropy, and various thixotropic fluid models explain industrial and natural flows. The gel breaking phase in drilling operations comes down to stress relaxation in the thixotropic fluid. In study [1], the authors conducted experiments with thixotropic fluid and reported the significant pressure drop under the steady rate. In [2] an indirect microstructural model for thixotropic fluids was overviewed, that related the rheology changes to a structural parameter. A model for thixotropic behaviour was proposed as a competition of gel building and gel breaking for capturing the oscillatory flow. A detailed study on flow startup with fluid enhanced with elastic stresses can be found in [3], where a numerical study analyses pressure behaviour for fluids of various rheology, including thixotropic fluid.

Specific applications of models with thixotropy to drilling comprise the fits of mud rheology measurements [4] and the matching of annular pressure drop after pumps start up [5]. The latter work tuned a gel breaking coefficient in the empirical closure for wall friction. Multiple analytical solutions for thixotropic non-Newtonian fluid are available in the literature for thixotropic behavior in pipe. For example, a steady analytical solution for pipe flow of thixotropic viscoplastic fluid was found [6]. The evaluation of steady flow [7] develops a particular case of study [6] and applies the specific closures for cement. In [8], the authors were interested in the transient solution for oscillating pressure for several thixotropic fluids. To our knowledge, the practical case of flow ramp-up in the pipe has not been considered analytically yet and we focus on it here.

This paper proposes a physics-based model to evaluate pressure changes in thixotropic fluid flow of a constant rate. We couple Houska model for thixotropy [9] with continuity and momentum equations. We build the approximate solution of that problem with a control volumes approach. Finally, the parametric study of analytical solution and the implementation of the model are discussed.

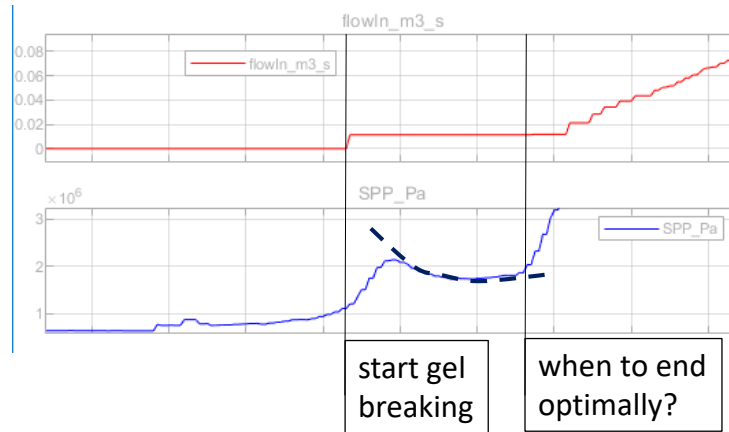


Fig. 1: Flow rate (in red) and pressure drop (in blue) during drilling operation. The dashed black line is for the model prediction.

2. Model

We consider a unidirectional laminar flow in the duct of constant cross-section A . The schematic of the flow in Figure 2 shows two axes with coordinates r and z . The third coordinate is either cartesian for the infinite planar duct ($m=0$) or polar for the circular pipe ($m=1$). The flow velocity has the only non-zero component u along z -coordinate.

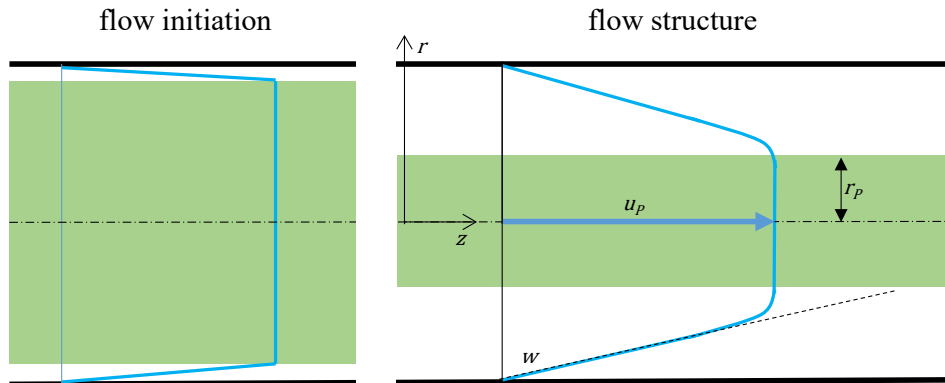


Fig. 2: Schematic of viscoplastic fluid flow in the duct/pipe. Plug zone is highlighted with green.

The fluid is incompressible and of constant density ρ , and is also viscoplastic. It satisfies the no-slip condition at duct walls. A viscoplastic flow contains plugs, where the stress is below the yield point τ . The plug moves as a solid body, while the rest of the fluid flows in the yielding zone. Figure 2 shows a typical flow structure for the duct flow with a plug in the middle. Due to the simple geometry, the only plug dimension is its size r_p .

The fluid is thixotropic. Prior to the start of the flow, the fluid stayed steady for an indefinitely long time. The plug has achieved the yield point τ_p . At the starting moment the flow rate immediately steps to the constant value Q . We assume, that after a short time the gel mass comes into motion and a thin gel layer next to the walls becomes broken (see the flow initiation in Figure 2). The further analysis of governing equations helps to evaluate the system state shortly after the flow ramps up.

Table 1: List of flow dimensional parameters.

| Parameter | Notation | Status | Depends on | Scale |
|--|-------------|---------|------------|--------------|
| time | t | | - | $DA/(2Q)$ |
| coordinate along pipe | z | | - | $D/2$ |
| coordinate in pipe section | r | | - | $D/2$ |
| steady flow rate | Q | scale | - | Q |
| duct diameter | D | scale | - | D |
| velocity z -component | u | unknown | r,t | $V = Q/A$ |
| yield point | τ | unknown | r,t | $\tau_{y,0}$ |
| rz -component of viscous stress tensor | τ_{rz} | unknown | r,t | $\tau_{y,0}$ |
| pressure | P | unknown | z,t | $\rho V^2/2$ |
| structural parameter | λ | unknown | r,t | 1 |
| rate constant related to gel build-up | k_1 | | - | $D/(2V)$ |
| rate constant related to gel breaking | k_2 | | - | 1 |

At first let us state a model for the unknown parameters from Table 1. A system of governing equations consists of a condition for steady flow rate from mass continuity, a z -component of momentum equations, and closures for fluid properties. Bingham model of constant viscosity μ covers the fluid behaviour. As in [9], we assume a thixotropic behaviour of the yield point τ_y , which depends on the structural parameter λ and varies between values $\tau_{y,0}$ and $\tau_{y,\infty}$. $\tau_{y,\infty}$ is the yield stress for fluid with complete gels breakdown, happening with the fluid set in motion for infinite time. $\tau_{y,0}$ is the yield point of fluid with fully developed gel. For the evolution of the structural parameter λ we use the approach from study [2].

$$\int_A u \, ds = Q \quad (1)$$

$$\rho \frac{\partial u}{\partial t} = -\frac{\partial P}{\partial z} + \frac{1}{r^m} \frac{\partial(r^m \tau_{rz})}{\partial r} \quad (2)$$

$$\tau_{rz} = \mu \frac{\partial u}{\partial r} + \text{sign}\left(\frac{\partial u}{\partial r}\right) \tau_y \quad \text{for } \tau_{rz} \geq \tau_y \quad (3)$$

$$\frac{\partial u}{\partial r} = 0 \quad \text{for } \tau_{rz} < \tau_y \quad (4)$$

$$\tau_y = \tau_{y,\infty} + \lambda (\tau_{y,0} - \tau_{y,\infty}) \quad (5)$$

$$\frac{\partial \lambda}{\partial t} = k_1(1 - \lambda) - k_2 \left| \frac{\partial u}{\partial r} \right| \lambda \quad (6)$$

Here m is geometry index, which is equal to 1 for planar duct and equal to 2 for circular pipe. Table 4 comprises other notations. Let us turn equations (1)-(3),(5),(6) to dimensionless form for the yielding zone with the scales from Table 1.

Together with scaling of equation (1),(3) and (6), the form of velocity profile is taken into account. The scaled system of governing equation has the following form:

$$\frac{A_p u_p}{A} + \int_{r_p}^1 u r^m dr = 1 \quad (7)$$

$$\frac{\partial u}{\partial t} = -\frac{\partial P}{\partial z} + \frac{1}{Re} \frac{1}{r^m} \frac{\partial}{\partial r} \left(r^m \left[\frac{\partial u}{\partial r} - Bm \tau_y \right] \right) \quad (8)$$

$$\tau_y = 1 + \delta\tau \lambda \quad (9)$$

$$\frac{\partial \lambda}{\partial t} = k_1(1 - \lambda) + k_2 \frac{\partial u}{\partial r} \lambda \quad (10)$$

Here A_p is a cross-section area of the plug and u_p is a plug velocity. Table 2 comprises dimensionless numbers in use.

Table 2: List of flow dimensionless parameters.

| Parameter | Notation | Definition | Case 1 |
|-----------------------|--------------|--|----------|
| Reynolds number | Re | $\frac{\rho V D}{\mu}$ | 1000 |
| Bingham number | Bm | $\frac{D \tau_{y,0}}{V \mu}$ | variable |
| yield point variation | $\delta\tau$ | $\frac{\tau_{y,0}}{\tau_{y,\infty}} - 1$ | 1 |

2.1. Problem analysis with control volumes approach

There are two control volumes to consider integrals of momentum equation (8). These control volumes are prisms of unit height. Table 3 shows their scaled parameters.

Table 3: Control volume parameters.

| Parameter | Planar geometry | Circular geometry |
|---------------------|-----------------|----------------------|
| m | 0 | 1 |
| Duct control volume | | |
| side wall S | 1 | 2π |
| base area A | 1 | π |
| Plug control volume | | |
| side wall S_p | 1 | $\max(0, 2\pi r_p)$ |
| base area A_p | $\max(0, r_p)$ | $\max(0, \pi r_p^2)$ |

For the duct segment between two cross-sections, the integral relates pressure gradient to velocity gradient and viscous stress τ_w at the wall as follows:

$$\frac{\partial P}{\partial z} = -\frac{S}{A Re} (w + Bm \tau_w) \quad (11)$$

Here w is the absolute value of the velocity gradient at the wall:

$$w = -\left. \frac{\partial u}{\partial r} \right|_{r=1} \quad (12)$$

The second specified control volume is a plug segment inside the duct segment. It has a cylindrical sidewall of area S_p and two cross-sections across the flow with area A_p . In the integral for this control volume, a pressure gradient can be expressed from equation (11) as:

$$-\frac{d(u_p A_p)}{dt} = \frac{A_p S}{A Re} \left(w + Bm \left(\tau_w - \frac{A S_p}{A_p S} \tau_p \right) \right) \quad (13)$$

The combination of equations (9) and (10) at the wall looks as follows:

$$\frac{d\tau_w}{dt} = k_1(1 + \delta\tau - \tau_w) - k_2 w(\tau_w - 1) \quad (14)$$

Equations (13) and (14) form a system of ordinary differential equations for w and τ_w , once the plug properties are known functions of w .

Due to a flow jump at $t = 0$ the multiple properties of the flow possess singularity, however the equations (13) and (14) provide an initial condition at the small time t as a following asymptotic:

$$w \sim \frac{Re}{S} \frac{1}{t} \quad (15)$$

The singularity of the solution at the start occurs due to fluid incompressibility. In reality, the acoustic pressure wave propagates along the duct and induces the flow, so the pressure drop has a phase of growth, until all fluid column comes into motion (see Figure 1). The fluid compressibility, acoustic wave and reproduction of pressure drop growth are out of scope of the model.

3. Solution

3.1. Solution in the plug zone

Regardless of the yielding zone evolution, there is continuous gelation in the plug. According to equations (4) and (6), the yield point of plug grows uniformly as follows:

$$\tau_p(t) = 1 + \delta\tau - (1 + \delta\tau - \tau_p(0)) \exp(-k_1 t) \quad (16)$$

3.2. Steady state solution in the yielding zone

The steady state statements of (13), (14) lead to the relation between final plug size and other flow properties. As eventually the plug achieves gel yield point, they are as follows:

$$w + Bm \left(\tau_W - \frac{1 + \delta\tau}{r_p} \right) = 0 \quad (17)$$

$$k_1(1 + \delta\tau - \tau_W) - k_2w(\tau_W - 1) = 0 \quad (18)$$

More details on steady state solution can be found in [6]. The final plug under the fixed conditions has the size as follows:

$$r_p = \frac{Bm (1 + \delta\tau)(Kw - 1)}{w (Kw - 1) + Bm (Kw - 1 - \delta\tau)} \quad (19)$$

$$K = \frac{k_2}{k_1}$$

The thixotropic fluid forms larger plug, than conventional Bingham fluid, because a gel build up eventually dominates in the regions with low velocity gradient. Coefficient K comprises balance between gel rates and flow velocity. Equation (19) evaluates, how effective can be gel breaking reduce the plug under steady flow rate.

3.3. Approximate solution under assumption of parabolic velocity profile in the yielding zone

In this section we build an approximate analytical solution with an additional assumption. For the yielding zone, fluid rheology model imposes the following conditions on velocity:

$$\left. \frac{\partial u}{\partial r} \right|_{r=r_p} = 0, \quad u|_{r=r_p} = u_p, \quad u|_{r=1} = 0 \quad (20)$$

Equations (7) and (20) complete the system of ordinary equations (13) and (14). Equation (11) obtains the pressure evolution from the flow parameters at the wall. The structural parameter is responsible for gel percentage. It is non-uniform in the yielding zone and changes between the value at the wall and 1. The minimal value of a structural parameter is linked to the yield point at the wall and comes from equations (9) and (14).

3.4. The case of planar duct with parabolic profile approximation

The proposed approach leads to the integration of (7), (13), (14), (20). Let us apply it to the case of the planar duct ($m=0$), while the solution of another case comes with longer expressions. The velocity profile in the yielding zone has the following form:

$$u(r, t) = \frac{3(1 - r)(1 + r - 2r_p)}{(1 - r_p)^2(2 + r_p)} \quad (21)$$

The plug velocity and the wall velocity gradient depend on the plug size as:

$$u_p = \frac{3}{2 + r_p} \quad (22)$$

$$w = \frac{6}{(1 - r_p)(2 + r_p)} \quad (23)$$

Figure 3 illustrates formula (23) with plug size versus velocity gradient at the wall. It is a purely geometrical constraint resulted from the mass conservation and the assumption on parabolic profile. The flow evolves from the large plug size to small towards steady state value, namely from right top corner of Figure 3 along blue curve toward the intersection with the red curve. According to equation (22), the plug gains velocity upon contraction. The plug velocity cannot exceed the value of 1.5, which corresponds to a fluid without a yield point. If the velocity gradient at the wall has the minimum value of 3, which corresponds to the plug absence and complete parabolic velocity profile.

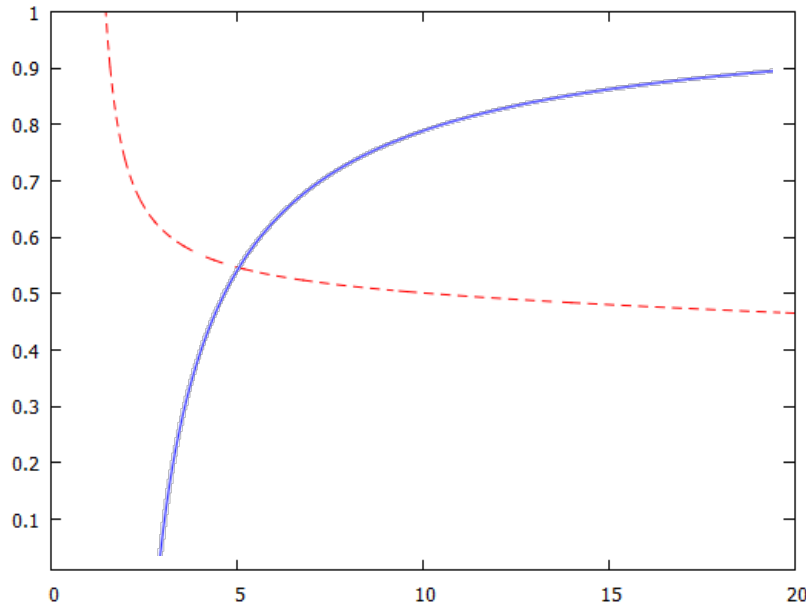


Fig. 3: Plug size vs velocity gradient at the wall for the Bingham fluid flow in the duct. The constrain due to parabolic profile assumption – blue line. The steady state solution– dash red line ($Bm = 5$, $K = 2$, $\delta\tau = 1$).

Equations (13),(14),(20)-(23) provide w defined in (12) as a function of time. Figure 4 shows evolution of velocity gradient at the wall for different Bingham numbers for “Case 1” in Table 1 and for thixotropy $\tau_p = 1$, $k_2 = 1$ and $k_1 \ll 1$. The initiated flow has a steep velocity gradient at the start, as predicted by the asymptotic (15). The sheared flow of the yielding zone invokes the gel breaking, and the zone expands. As a result, the velocity gradient decreases and pressure drop falls. Simultaneously the plug becomes smaller, while gaining velocity. For different Bingham numbers the flow stabilizes at the well-known solution of steady state Bingham fluid flow. For higher Bingham numbers (less viscous fluid or higher yield point) the flow stabilization takes shorter time, and the final plug will be larger.

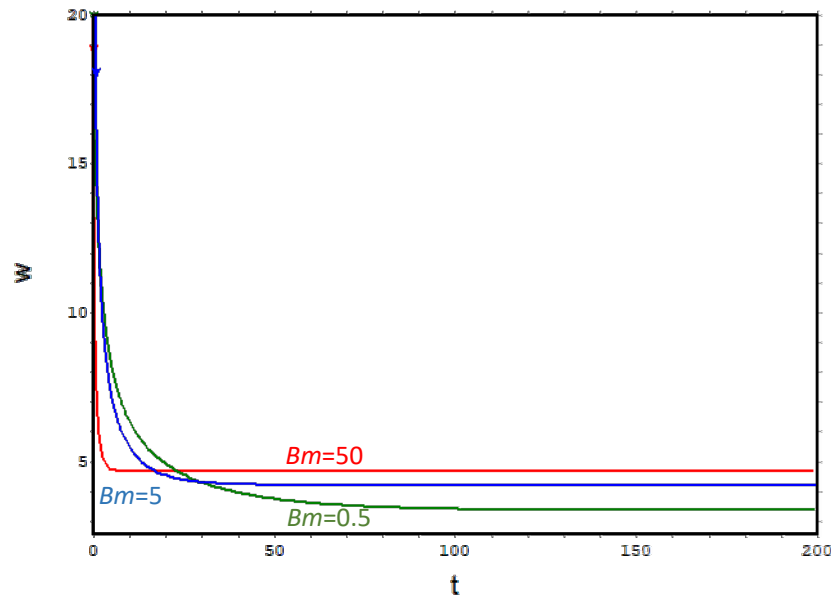


Fig. 4: Velocity gradient at the wall versus time for several Bingham numbers for thixotropic fluid flow in the duct after sudden flow rate ramp up.

3. Discussion

The time of stabilization is an important value in industry, particularly in drilling operations. It signifies the gel breaking stage. Having known its value, the processes sensitive to gel presence can be properly planned and automated. For example, in drilling operation the presence of gel significantly increases the pressure drop (see Figure 1), so that the system has to withstand the high pressures or execute under the lower flow rate. As the plug approaches to its steady size, the operation might get acknowledged on the accomplished gel breaking phase. The approximate solution enables an implementation in real time. It is important to notice, that a steady flow of viscoplastic fluid does not lose the plug completely, though the thixotropy effect reduces the plug size until the stabilization is achieved.

Typically, in the advanced rheology measurements gel parameters are evaluated in a thin sheared flow with step-wise changes of velocity gradient. In the task considered above, the sheared flow was non-uniform and the thixotropy gradually changed it. The proposed solution enables the scaling of gel parameters to the full-size flow. As result we observe the decrease of the yield point, so the thixotropy effect sustains flow lubrication up to flow stabilization.

4. Conclusion

The model for the transient thixotropic flow in the duct is based on momentum equations coupled with the indirect thixotropic Heschel-Bulkley fluid model. A sudden flow rate step invokes the flow, and a thixotropic effect makes the flow transient. The flow has plug and yielding zones; their sizes significantly change up to the flow stabilization. A simple geometry and an effective assumption on a parabolic profile allow an analytical solution. The evolution of velocity gradient at the wall defines all the other flow parameters. The analysis shows, how the gels breaking develops in a large-scale flow with respect to fluid properties. The solution finds its application in industrial processes, where the reduction of gels in a flow is important.

5. Acknowledgement

Thanks should also go to my colleague Roger Aragall, who brought more clarity to the manuscript with detailed discussion of the problem.

References

- [1] M. P. Escudier and F. Presti, “Pipe flow of a thixotropic liquid,” *Journal of Non-Newtonian Fluid Mechanics*, no. 62, pp. 291-306, 1996.
- [2] A. Mujumdar, B. N. Antony and A. B. Metzner, “Transient phenomena in thixotropic systems,” *Journal of Non-Newtonian Fluid Mechanics*, vol. 102, no. 2, pp. 157-178, 2002.
- [3] C. O. Negrão, A. T. Franco and L. L. Rocha, “A weakly compressible flow model for the restart of thixotropic drilling fluids,” *Journal of Non-Newtonian Fluid Mechanics*, vol. 166, no. 23-24, pp. 1369-1381, 2011.
- [4] P. R. d. S. Mendes, “Modeling the thixotropic behavior of structured fluids,” *Journal of Non-Newtonian Fluid Mechanics*, vol. 164, pp. 66-75, 2009.
- [5] J. Maxey and D. Jamison, “Modeling Gel Breakdown for Improved Pressure Control,” in *AADE Fluids Technical Conference and Exhibition*, Houston, 2012.
- [6] A. Ahmadpour and K. Sadeghy, “An exact solution for laminar, unidirectional flow of Houska thixotropic fluids in a circular pipe,” *Journal of Non-Newtonian Fluid Mechanics*, vol. 194, pp. 23-31, 2013.
- [7] R. De Schryver and G. De Schutter, “Insights in thixotropic concrete pumping by a Poiseuille flow,” *Applied Rheology*, no. 30, pp. 77-101, 2020.
- [8] D. Pritchard, A. I. Croudace and S. K. Wilson, “Thixotropic pumping in a cylindrical pipe,” *Physical Review Fluids*, vol. 5, no. 013303, 2020.
- [9] M. Houska, “Engineering Aspects of the Rheology of Thixotropic Liquids,” Czech Technical University, Prague, 1981.

Appendix

Table 4: Table of notations.

| Notation | Description |
|-------------------|--|
| Greek | |
| $\delta\tau$ | yield point variation |
| λ | structural parameter |
| μ | viscosity |
| ρ | density |
| τ_y | yield point |
| τ_w | yield point at the wall |
| τ_{rz} | stress tensor component |
| $\tau_{y,0}$ | yield point for complete gel breakdown |
| $\tau_{y,\infty}$ | yield point for complete gel buildup |
| Latin | |
| A | pipe/duct cross-section area |
| A_p | plug cross-section area |
| Bm | Bingham number |
| D | diameter of the pipe/duct |
| k_1 | gel building rate |
| k_2 | gel breaking rate |
| m | geometry index |
| P | pressure |
| r | coordinate across the pipe/duct |

| | |
|-------|--|
| Re | Reynolds number |
| S | wall surface area |
| S_p | plug surface area |
| t | time |
| Q | flow rate |
| u | velocity |
| w | opposite velocity gradient at the wall |
| z | coordinate along the pipe/duct |

The equation (14) can be effectively integrated to express yield point at the wall explicitly:

$$\frac{d\tau_w}{dt} = -f(t)(\tau_w - 1) + c, \quad f(t) = k_1 + k_2w, \quad c = k_1\delta\tau \quad (24)$$

$$\tau_w = 1 + \exp\left(-\int_0^t f dt\right) \left(\tau_{w,0} - 1 + c \int_0^t \exp\left(\int_0^i f di\right) dt \right) \quad (25)$$

Particularly for a constant velocity gradient:

$$\tau_w = \exp(-ft) (\tau_{w,0} - 1) + 1 + \frac{c(1 - \exp(-ft))}{f} \quad (26)$$